



On the transport mechanism of rockfalls and avalanches  
by Jeffrey Michael Lacy

A thesis submitted in partial fulfillment of the requirements for the degree OF Master of Science in  
Engineering Mechanics  
Montana State University  
© Copyright by Jeffrey Michael Lacy (1989)

**Abstract:**

In this thesis, a numerical model of a granular shear flow is developed. This model is two-dimensional and assumes the shearing granules to be identical, smooth, semi-elastic circular disks. The field containing these disks is bounded on the top and bottom by solid blocks of disks with the same properties. The field is bounded on the right and left by periodic boundaries. The top boundary block has an assigned horizontal velocity and overburden mass, and is unconstrained in the vertical direction. The base boundary block is immobile and does not permit scour.

The numerical model is then used to test the hypothesis that, for large overburden pressures, collisions in the shearing region occur involving more than two particles, and that these multi-particle collisions act to reduce the shear strength of the dilatant granular flow.

Flows were modeled for a variety of shear speeds and overburden pressures. Results of these simulations show that, although multi-particle collisions do occur with increasing frequency as overburden is increased, they do not have any significant effect on the shear strength of the granular flow. Therefore, this hypothesis is rendered invalid.

ON THE TRANSPORT MECHANISM OF  
ROCKFALLS AND AVALANCHES

by

Jeffrey Michael Lacy

A thesis submitted in partial fulfillment  
of the requirements for the degree

of

Master of Science

in

Engineering Mechanics

MONTANA STATE UNIVERSITY  
Bozeman, Montana

April 1989

N378  
L1185

APPROVAL

of a thesis submitted by

Jeffrey Michael Lacy

This thesis has been read by each member of the thesis committee and has been found to be satisfactory regarding content, English usage, format, citations, bibliographic style, and consistency, and is ready for submission to the College of Graduate Studies.

4/14/89  
Date

Jim Dent  
Chairperson, Graduate Committee

Approved for the Major Department

4/14/89  
Date

Heather E. Ray  
Head, Major Department

Approved for the College of Graduate Studies

April 18, 1989  
Date

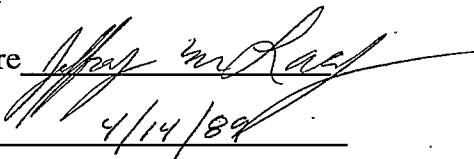
Henry L. Parsons  
Graduate Dean

## STATEMENT OF PERMISSION TO USE

In presenting this thesis in partial fulfillment of the requirements for a master's degree at Montana State University, I agree that the Library shall make it available to borrowers under rules of the Library. Brief quotations from this thesis are allowable without special permission, provided that accurate acknowledgment of source is made.

Permission for extensive quotation from or reproduction of this thesis may be granted by my major professor, or in his absence, by the Dean of Libraries when, in the opinion of either, the proposed use of the material is for scholarly purposes. Any copying or use of the material in this thesis for financial gain shall not be allowed without my written permission.

Signature

A handwritten signature in cursive script, appearing to read "Jeffrey M. Reed", written over a horizontal line.

Date

A handwritten date "4/14/89" written over a horizontal line.

## TABLE OF CONTENTS

	Page
LIST OF TABLES . . . . .	vi
LIST OF FIGURES . . . . .	vii
ABSTRACT . . . . .	ix
1. INTRODUCTION . . . . .	1
2. THE CURRENT STATE OF KNOWLEDGE . . . . .	4
Review of Previous Work . . . . .	4
The Problem . . . . .	10
3. THE INVESTIGATION . . . . .	12
Numerical Simulation . . . . .	12
The Code . . . . .	13
Data Input and Parameters . . . . .	14
Run Initialization . . . . .	18
Virtual Elements and Periodic Boundaries . . . . .	18
Contact Mechanics . . . . .	21
Contact Parameter Flags . . . . .	24
Subroutine IMPACT . . . . .	25
Subroutines TYMJUMP and TIMER . . . . .	26
Positions, Velocities, and Forces . . . . .	27
Output and Graphics . . . . .	28
Simulation Accuracy and Discussion . . . . .	28
Experimental Procedure . . . . .	31
4. RESULTS AND CONCLUSIONS . . . . .	32
Results . . . . .	32
Conclusions . . . . .	60
Suggestions for Further Research . . . . .	61

TABLE OF CONTENTS--Continued

	Page
LIST OF REFERENCES . . . . .	63
APPENDICES . . . . .	67
Appendix A--Listing of the Code SNOFLO . . . . .	68
Appendix B--Examples of Data from the SNOFLO Simulation . . . . .	79

## LIST OF TABLES

	Page
1. Shear Speed = 5000 d/s, Overburden Varying . . . . .	80
2. Shear Speed Varying, Overburden = 2 kPa . . . . .	81
3. Shear Speed Varying, Overburden = 15 kPa . . . . .	82
4. Shear Speed Varying, Overburden = 32 kPa . . . . .	84

## LIST OF FIGURES

	Page
1. Contact Force and the Overlap Delta . . . . .	15
2. Shear Field Initialization . . . . .	17
3. Virtual Particles and the Virtual Field . . . . .	19
4. Particle Contacts Across a Periodic Boundary . . . . .	20
5. Particle Moving Through the Right Periodic Boundary . . . . .	20
6. Particle Passing Through the Left Periodic Boundary . . . . .	21
7. Contact Force vs. Overlap for a Binary Collision . . . . .	22
8. Contact Force vs. Overlap for a Multi-Particle Collision . . . . .	23
9. Impact Angle Theta . . . . .	26
10. Stress Ratio S/N vs. Shear Velocity at 2 kPa . . . . .	36
11. Stress Ratio S/N vs. Shear Velocity at 15 kPa . . . . .	37
12. Stress Ratio S/N vs. Shear Velocity at 32 kPa . . . . .	38
13. Stress Ratio vs. Shear Velocity Derived from the Theory of Richman and Chou	39
14. Stress Ratio vs. Shear Velocity from Dent's Numerical Model . . . . .	40
15. Stress Ratio vs. Shear Velocity from Hanes and Inman . . . . .	41
16. Stress Ratio vs. Shear Velocity from Savage and Sayed . . . . .	42
17. Stress Ratio vs. Shear Velocity from Bridgwater . . . . .	43
18. Flow Depth vs. Overburden . . . . .	47
19. Stress Ratio vs. Overburden . . . . .	48

LIST OF FIGURES--Continued

	Page
20. Fraction of Time There are Contacts vs. Overburden . . . . .	49
21. Time Fraction of Contacts that are Multiple vs. Overburden . . . . .	50
22. Shear Fraction M/S vs. overburden . . . . .	51
23. Flow Depth vs. Shear Velocity at 2 kPa . . . . .	53
24. Flow Depth vs. Shear Velocity at 15 kPa . . . . .	54
25. Flow Depth vs. Shear Velocity at 32 kPa . . . . .	55
26. Shear Fraction M/S vs. Shear Velocity at 2 kPa . . . . .	57
27. Shear Fraction M/S vs. Shear Velocity at 15 kPa . . . . .	58
28. Shear Fraction M/S vs. Shear Velocity at 32 kPa . . . . .	59
29. Listing of the Code SNOFLO . . . . .	69

## ABSTRACT

In this thesis, a numerical model of a granular shear flow is developed. This model is two-dimensional and assumes the shearing granules to be identical, smooth, semi-elastic circular disks. The field containing these disks is bounded on the top and bottom by solid blocks of disks with the same properties. The field is bounded on the right and left by periodic boundaries. The top boundary block has an assigned horizontal velocity and overburden mass, and is unconstrained in the vertical direction. The base boundary block is immobile and does not permit scour.

The numerical model is then used to test the hypothesis that, for large overburden pressures, collisions in the shearing region occur involving more than two particles, and that these multi-particle collisions act to reduce the shear strength of the dilatant granular flow.

Flows were modeled for a variety of shear speeds and overburden pressures. Results of these simulations show that, although multi-particle collisions do occur with increasing frequency as overburden is increased, they do not have any significant effect on the shear strength of the granular flow. Therefore, this hypothesis is rendered invalid.

## CHAPTER 1.

## INTRODUCTION

Rockslides and avalanches continue to be studied vigorously by scientists and engineers for very good reason. They are some of the least predictable, most violent, costly, and deadly phenomena Nature has to offer. Extremely large rockfalls and avalanches, though not nearly as common as the smaller ones, deserve extra attention. This is not only due to the amazing catastrophe they can create, but also because of a phenomenon exhibited by them that does not yet have any satisfactory explanation. Simply put, large events move faster and travel further than current accepted knowledge allows. A few examples illustrate the point.

The rockfall of Nevados Huascarán, Peru in 1970 buried the entire town of Yungay, killing more than 18,000 people in about three minutes. Its average velocity was calculated to be about 280 km/hr. To get an idea of the violence of this event, Plafker and Ericksen (1978) calculated from the size of its impact crater that a 65 tonne boulder found in a field later must have been thrown four kilometers, indicating a launch velocity of about 1000 km/hr. On March 6, 1898, near the village of Glarus, Switzerland, a snow avalanche started near the summit of Vorderglarnisch (Fraser, 1978). A little less than a minute later, the Great Glarnisch avalanche had dropped a vertical distance of 5750 feet, and run  $4 \frac{1}{3}$

miles from its starting point, including 1 1/2 miles of level valley floor. It had an average velocity of 225 mph.

December 27, 1938 saw a huge avalanche sweep down the Shiai-Dani chute in the Kurobe Gorge in northern Japan (Shimuzu et al, 1980). It hit a four story barracks of semi-underground construction, full of sleeping construction crewmen. The third and fourth stories were blown off the rest of the building, launched over a 20 m (66 ft) ridge, and hurled 600 m (well over 1/3 of a mile) across the Gorge. They, and the men inside, were smashed on the far-side wall of the Gorge. The first and second stories were simply crushed. In all, 84 men were killed.

On January 26, 1986 a similar, though probably smaller avalanche hit the village of Maseguchi in Northern Japan, killing thirteen people and destroying eleven homes (Yasue et al, 1987).

On September 11, 1881, a large rockslide started above the village of Elm, in Switzerland (Hsu, 1978). In about forty seconds, it travelled two kilometers, burying the village of Untertal and partly destroying Elm. Its average velocity was estimated at 300 km/hr.

The incredible speeds and runout distances of large events such as these have puzzled researchers and generated much controversy for at least the last three decades. Unfortunately, the very aspect of these phenomena which make them so very interesting -- their extreme violence -- also makes accurate measurements of their internal processes and mechanics virtually impossible. The transport mechanism of the great slides and avalanches, and why they reach such incredible speeds, though much modeled and hypothesized about, remains unknown. Yet these events will continue to occur around the

world in the future as they have in the past, making a better understanding of their behavior not only academically interesting but socially imperative, especially as people move to live and play more and more in the mountainous regions of the world.

In this paper, flow avalanches, which consist mainly of a dense core of flowing snow, are to be distinguished from powder avalanches, which have no such core and resemble more closely in their behavior turbidity currents than rockfalls. For the remainder of this paper the word "avalanche" can be taken to mean "flow avalanche" unless indicated otherwise. Also occasionally rockfalls will be referred to as "sturzstroms" after Hsu (1975) as this seems to be more descriptive of the debris flow aspect we are interested in than "rockfall" or "rockslide".

## CHAPTER 2

### THE CURRENT STATE OF KNOWLEDGE

#### Review of Previous Work

Research concerning rockslides and that of avalanches have generally been held separate from each other, although in many respects they are very similar events. Both show the following characteristics regularly, indicating that a similar mechanism drives them both. These characteristics also serve as a guide for researchers, since any hypothesis concerning sturzstroms and large avalanches must take them into account. These are (Davies, 1982):

1. Material in the final deposit is in the same sequential order as it was initially. In material of different colors, there is sometimes distinct longitudinal banding as well.
2. In Sturzstroms, shattered rock fragments remain close together, creating a "three-dimensional jigsaw" effect.
3. In the final deposit there are usually distal ridges, indicating a sudden stop.
4. There is a very strong similarity between deposits of events on earth and those on the moon and Mars, indicating the same mechanism is at work.
5. The size effect: Velocity and runout distance increase with the volume of the event, indicating a corresponding decrease in internal friction.

The serious study of sturzstrom behavior began with Albert Heim and his study of the Elm event mentioned above (Hsu, 1978). He proposed that the debris flowed rather than slid, and was met with some considerable resistance from his peers. In his 1932 paper, he suggested a mechanism for this flow. When any particle has a higher velocity than its forward neighbor, it collides with that neighbor and is not allowed to pass. Energy is transferred to the slower particle through the impact, which in turn collides with another particle. In this way, the sequential order of the flow is preserved and the kinetic energy of the fall is maintained, the only loss of internal energy of the flow being due to inelasticity of particle collisions. This model also satisfies criterion 2, the jigsaw effect, in that fragments of a broken clast would not be able to separate from each other.

In 1965 P. E. Kent proposed an entirely different mechanism. He stated that during the initial fall of rock, air is trapped beneath it. As this air rushes out of the rock mass it fluidizes the particles, thus relieving the interparticle frictional forces and allowing great speed.

Shreve, in 1968, proposed a "hovercraft" mechanism which enjoyed widespread popularity for a time. From his study of the Blackhawk slide, he figured that if a debris flow hit a suitable jump, it would compress a volume of air beneath it, which, due to scale effects, would not be able to escape quickly. The rock mass would then slip on a frictionless air cushion, thus reaching high velocity.

Guest (1971), and Howard (1973) found that rockfall deposits on the moon and Mars were very similar to those being studied on earth, lending serious doubt as to the validity of the air based theories of Kent and Shreve. Then Hsu (1975) and Erismann (1979) discredited the air layer concept completely with excellent arguments, the most

notable being first, the work of Guest and Howard; second, the fact that a volume of air behind a jump is not compressed under a moving "sheet" unless that sheet decelerates considerably (to near stop) while airborne over the volume to be compressed; third, the need for another mechanism to get the rock mass moving fast enough to become airborne from a small jump in the first place; and fourth, that the observed deep gouging of soft earth by sturzstroms is not possible if the flow doesn't actually touch the ground.

Hsu (1975) went on to link Heim's ideas with Bagnold's 1954 work on granular flow in an interstitial fluid. Hsu postulated that highly energetic intergranular dust in a rockfall could serve as Bagnold's interstitial fluid, with or without the presence of air.

From his work on the Kofels slide, Erismann (1979) proposed that high overburden pressures and the heat of friction at the base layer could cause a slide to self-lubricate either by the melting of base layer rock, producing a liquid lubricant, or by dissociation of basal rock (depending on rock composition) to produce a gas-dust lubricant. There is solid evidence for this happening in one case, but lack of evidence in any other leads one to conclude that while this mechanism is thermodynamically feasible, it does not play a great role in the vast majority of large events.

McSaveney (1978) noted that Bagnold's granular shear theory required no interstitial fluid to work, removing any theoretical need for Hsu's interparticle dust.

In 1981, T.R.H. Davies proposed that sturzstroms owe their nature to pure mechanical fluidization. In this model, particles in the flow get enough kinetic energy to become statistically separated; and particle-particle interaction is only through brief impacts. In this state, the flow behaves much like a molecular fluid, and notably, much like Heim proposed in 1932.

In the West, analysis of snow avalanches began with the work of Voellmy in 1955, who proposed that an avalanche could be treated as an open channel, incompressible, steady-state fluid flow. His expressions remain in use in many areas as the foremost calculational tool for the prediction of avalanche danger. However, the method does have limitations. For example, it requires that the point where run-out begins be chosen, rather subjectively, by the analyst. And it requires a choice of a variety of snow and flow parameters including flow density, flow height, and mean deposition depth, which vary with snow and weather conditions, and with the researcher reporting them. There are also some theoretical drawbacks. In the words of LaChapelle and Lang (1980),

"Formally, The Voellmy method is severely limited because it is invalid for movements with local accelerations, applies to internal snow flow and not the avalanche front, does not describe motion of the airborne dust cloud, and requires the equation of continuity be met. Avalanche observations in the real world, including ours, seldom meet these criteria."

Over the years, several other fluid-based models have been proposed, ranging from Salm's (1966) center of mass motion equations, to Dent and Lang's (1983) biviscous modified Bingham fluid proposal, to the continuum mechanical approach of Norem, Irgens, and Schieldrop (1986).

While these methods can be used to model quite accurately the external features of avalanche events, they rely on such parameters as the kinetic and turbulent coefficients of friction, viscosity, flow height, or locking shear stress, which are impossible to determine for any given event until after it has happened, if at all. Since these parameters must usually be back calculated from the very expressions they are used in, the models are reduced to empirical relationships which may not have any connection with the actual mechanics of the event. Also, because of the wide range of values of these coefficients,

the predictive value of these models is limited.

In 1980, A.I. Mears published a study of 45 avalanches in which he found no correlation at all between the run-out distance and slab height, or between the run-out distance and the slope of either the track or the run-out zone. All three parameters figure prominently in many of the fluid models. He also found that 80 to 90 percent of dry slab avalanche debris consisted of snow fragments larger than 5 cm in diameter. He went on to propose a granular shear flow mechanism such as that studied by Bagnold (1954).

In 1987, Hutter, Szidarovsky, and Yakowitz modeled avalanche flow assuming a granular shear flow mechanism proposed by Jenkins and Savage (1983). They found that it was most realistic to assume that a near-bed layer of material is fluidized, carrying on it the nearly passive load of the bulk of snow. It will be interesting to remember later that the work of Jenkins and Savage, and thus that of Hutter et al, is based on their explicit assumption that particle interaction in the fluidized region is strictly through binary collisions.

Currently, researchers in both the fields of rockfalls and snow avalanches are coming to embrace the concept of near-bed fluidization as the major transport mechanism. In this model, as a falling mass of rock or snow gains velocity, granules or clasts near the base of the flow, where the shear rate is highest, gain enough energy to separate, dilating that layer. The material above this fluidized layer is carried passively and deforms slowly relative to the highly activated shear region. The expanded base layer has very little shear strength, allowing the low observed apparent coefficient of friction of large events. This model satisfies the observed behavior characteristics as follows.

Sequential order of the material in the final deposit is maintained since the bulk of the material is carried relatively passively by the highly activated shear layer. The shearing layer entrains material from the leading edge of the flow and deposits it at the rear, accounting for the thin smear on the bottom of the final deposit noted by Dent (1982).

The "three dimensional jigsaw" effect is also due to the fact of the slowly deforming bulk of the flow. Since there is little or no turbulence in the majority of the material, clasts broken in the original fall will remain close together during the runout.

Lateral ridges in the distal regions of the final deposit form due to the collapse of the dilated shear layer. As the flow loses speed in the run-out, the front-most regions of the dilatant base layer will lose enough energy to collapse, suddenly increasing friction forces and decelerating quite rapidly. Material behind the collapsed region will collide with it and try to ride up over the slower material before losing momentum itself, causing a series of lateral ridges in the distal areas of the deposit.

The similarity of terrestrial events to those on the moon and Mars arises because all that is required for this mechanism to work-- gravity and some bulk material to flow-- is available at all three sites.

The size effect, wherein velocity and runout distance increase with the volume of the event, is not necessarily explained by this model. It appears that although the model is basically correct, there is an additional mechanism at work within the shearing region which has not yet been accounted for.

### The Problem

The size effect observed in large avalanches and sturzstroms is not explained effectively by the current fluidized base layer theory. Direct radar measurements of avalanche velocities by Gubler (1987) and observations by many others leave no doubt about the veracity of this phenomenon. The loss of internal energy of both sturzstroms and avalanches decreases as the volume of the event increases, yielding higher velocities and longer run-out distances for large events.

Although a dilatant base layer does reduce the apparent friction of a granular flow, it should not, according to present knowledge, do so in the manner observed. As the mass of a flow increases, there should be some jump in velocity as the critical mass for bed fluidization is reached. Then as mass is added, the dilatant layer should be compressed, shortening the mean free path of the fluidized particles, and increasing the shear strength of the layer, slowing the flow. McSaveney (1978) stated the problem like this.

"With increasing thickness of avalanche, the mean free path of the clasts shortens, and hence the frequency of collisions increases with thickness as well as with number of clasts. Large, thick avalanches might thus be expected to lose energy more rapidly than smaller, thinner ones, and thus have higher internal friction."

Currently, a mechanism that would resolve this contradiction between expectation and observation is being sought. Dent, in 1986, proposed the following hypothesis:

As a fluidized bed is compressed by increasing overburden, collisions between particles cease to be purely binary, and multiple collisions begin to occur. These multiple collisions form, for the briefest of moments, chains of particles, or microstructures, in the layer which have high axial strength and low or negligible shear strength. Cumulatively, these microstructures could help support the overburden pressure without much affecting

the shear strength of the layer, thus effectively reducing the ratio of shear to normal stress and reducing the apparent friction of the overall event. To state this concisely, this hypothesis predicts that

1. A fluidized bed compresses as overburden is added.
2. This compression causes multiple-contact microstructures to form.
3. These micro structures present a lower ratio of shear resistance/normal force than do binary collisions alone.
4. These structures form frequently enough to reduce noticeably the overall shear ratio, and thus reduce the apparent friction of the flow.

The purpose of this research is to test the predictions of this hypothesis and discover if this is a viable explanation for the size effect.

## CHAPTER 3

### INVESTIGATION

The investigation of this hypothesis was a numerical (computer) simulation of a shearing system of particles. The experiment was designed both to observe whether microstructure chains actually do form, and to measure their effect on the shearing system as a whole.

#### Numerical Simulation

The first phase of research was to build a computer simulation of the basal shear layer. The model is a two dimensional field of disks, bounded on the bottom by a row of immovable disks and on the top by a row of disks with an assigned horizontal velocity and overburden mass. At the left and right hand edges of the field there are periodic boundaries, meaning simply that whatever exits the field on one side will reenter on the other, with the same altitude and velocity. All particles are assigned a diameter, mass, hardness (spring coefficient), and elasticity (coefficient of restitution).

The simulation follows the exact paths of all the disks in the field, calculating the position, velocity, and acceleration of each over small time increments. Accelerations only occur when a particle is in contact with any other. This simulation is different from that of Hutter et al (1987) and the grain flow simulation of Campbell (1982) in that those

models assumed only binary collisions between particles and simply calculated the results of each contact, where this model follows the true path of particles, allowing any number particles to contact at once.

### The Code

The following section is a detailed description of the numerical simulation code. SNOFLO was written by the author in June, 1988 in Fortran on a VAX/VMS network system.

The code will be discussed by its sections in the following order:

1. Data and parameter input
2. Run initialization
3. Virtual elements and periodic boundaries
4. Contact mechanics
5. Contact parameter flags
6. Impact subroutine
7. Time jumping subroutines
8. Positions, velocities and forces
9. Output and graphics
10. Simulation accuracy and discussion

This order is used because it follows the flow of the code itself. A copy of the code is listed in Appendix A for more rigorous inspection.

### Data Input and Parameters

Run parameters are read from the data file CNTRL.DAT. Reads are unformatted --only the parameter order is important. The parameters, in the order they appear in CNTRL.DAT are:

```
RESTRT,GRAPH  
K1, K2, D, M, G, MTOP  
NHT, NWID, TWID, VXT  
STEP, LOOP, TIME
```

Where the first row contains I/O flags; the second the physical properties of the material chosen, in the desired units; the third row contains array and field building information; and the fourth has time parameters. Each parameter and its function will be discussed in turn.

The RESTRT flag indicates whether or not the ensuing run is new or the continuation of an old one. If RESTRT equals 1, particle positions and velocities, along with the elapsed time and total number of cycles, are read from a formatted file RESTART.DAT, which was created by the run which is to be restarted. A new restart file is created at every output interval during a run. This ensures that in the event of an accidental abort or interruption very little time will be wasted recovering old ground. If RESTRT equals 0 a brand new array of particles is created.

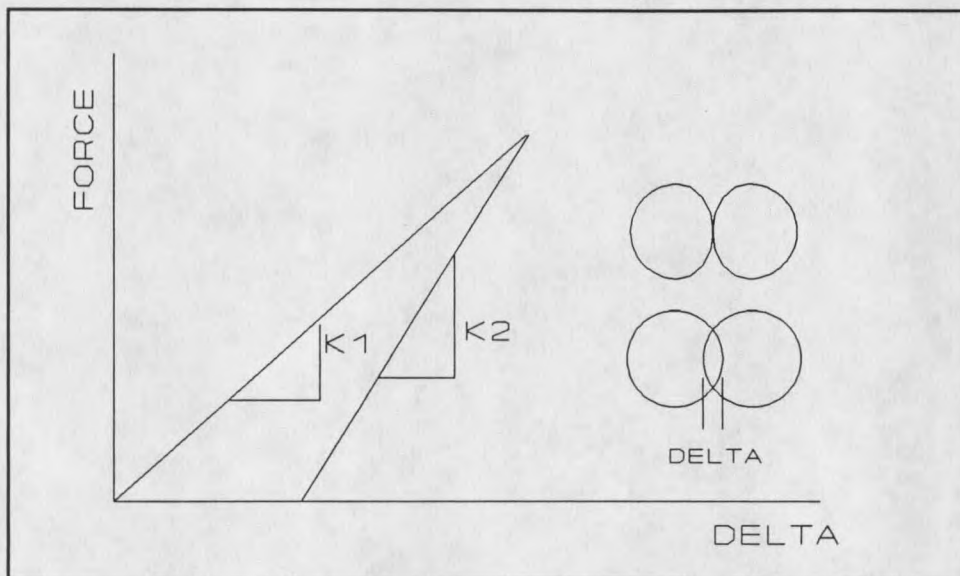
GRAPH is a graphics flag. If this is set to one, then at each output interval a formatted file PIC.DAT is created, into which is fed the position of every particle (real or virtual) that is either within or is touching the field boundaries. The subroutine PICTURE is then called, which reads the particle positions and employs a series of DISSPLA commands to create a META.DAT graphics file. This allows "pictures" of the particle field to be taken at desired intervals. This visual information can be especially useful in helping

the observer to understand how the simulation is progressing. With properly timed graphics intervals, one may use a movie camera to take single frame pictures of a run as it progresses, creating an animated film of the simulated shear region. This was done, and although it is a very time consuming process, the resulting film yields valuable information about the nature of the fluidized system of particles.

$K_1$  and  $K_2$  are the spring constants of the particles and represent their "hardness." In a binary collision  $K_1$  is the approach constant, while  $K_2$  is the retreat constant. The ratio  $K_1/K_2$  is in real time the coefficient of restitution of the material  $e$ . See Figure 1.

Figure 1

Contact Force and the Overlap Delta



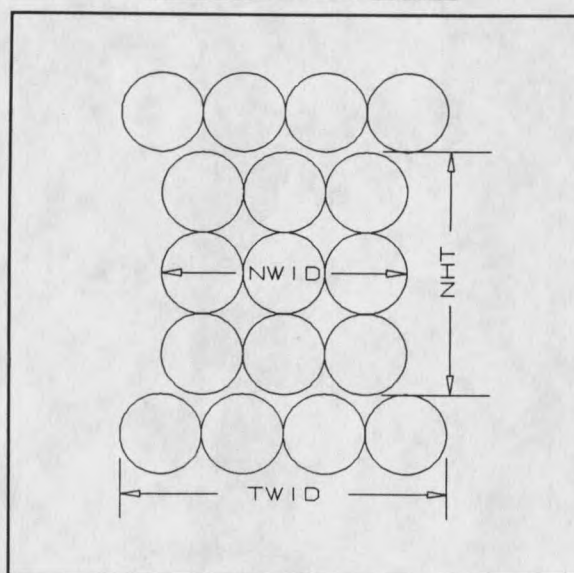
In the numerical simulation, time is not continuous, but is discretized into finite steps. This causes the ratio  $K_1/K_2$  to become less than the actual coefficient of restitution. The amount of variation is directly dependent on the size of the time step chosen. To find  $K_1/K_2$  for a desired  $e$ , a field was set up such that two particles could collide without

interference. Then the ratio  $K1/K2$  was adjusted to achieve the desired rebound velocities calculated from the desired coefficient of restitution. It was found that for a time step of  $10^{-7}$  sec, and a coefficient of restitution of 0.7 the ratio of  $K1/K2$  was 0.45. It was found that the coefficient of restitution is stable for impact velocities spanning four orders of magnitude. The relationship between  $K1$ ,  $K2$ , and  $DELNOT$  becomes more complicated during multiple collisions. This event will be discussed in detail later.

The diameter and mass of the particles are  $D$  and  $M$ , respectively. In this model, all particles are of uniform size and mass. While this gives quite useful results, it would be interesting to see the results of a similar model with randomly sized particles. This is recommended for further investigation.

$G$  is the gravitational acceleration, scaled to whatever system of units the investigator has chosen. Gravity does not act on the free particles in the array. It only acts on the upper block of particles. This upper block represents the bottom surface of the slowly deforming overburden load. Hence it is assigned mass  $MTOP$ , which represents the mass of the snow or rock above the field. To find overburden pressure, one must find the force  $MTOP * G$ , and divide by the field area  $TWID * D^2$ .

The next row of parameters define the size of the array to be used and the width of the field to which it is confined. The free particles are initialized in a rectangular matrix.  $NHT$  gives the number of rows of the matrix, and  $NWID$  gives the number of columns.  $TWID$  is the number of particles in both the top and bottom boundary blocks and hence also gives the width of the field in diameter lengths. After initialization, the field is set up as in Figure 2.

Figure 2Shear Field Initialization

VXT is the assigned horizontal velocity of the top block. This remains constant, although the vertical position and vertical velocity are free to change.

The last line of CNTRL.DAT gives the time parameters of the code. STEP is the size of the time increment to be used while calculating collision results. This may be made small at expense of much CPU time, or larger at the expense of accuracy. For this work a time step of  $10^{-7}$  was used and yielded good results. LOOP is the output time interval. At the end of each interval, all output files are updated and graphics are created. TIME is time interval for which the simulation is to run. Although this can be made arbitrarily large so that runs may be aborted when the investigator chooses, this is not recommended. Without a logical stop, all graphics files will be lost. Also TIME should be kept small until

an investigator is familiar with the properties of the simulation--one second of flow time averages 10 to 13 hours of CPU time on the VAX.

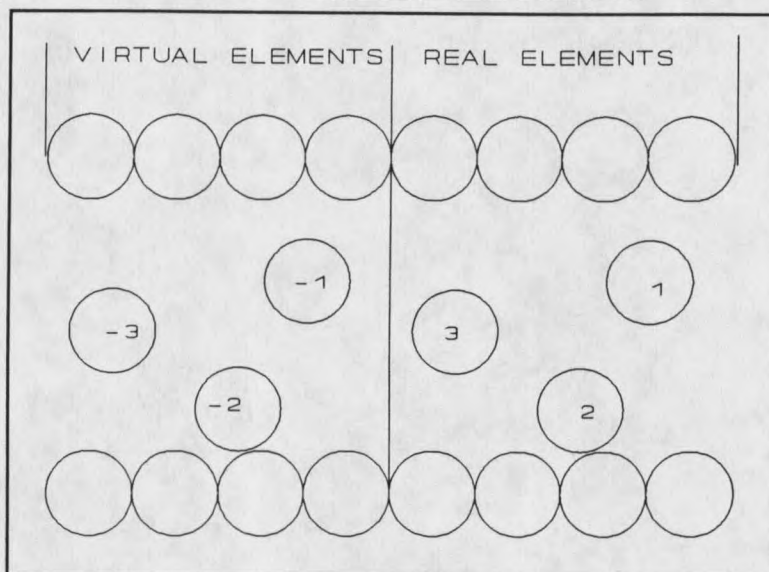
### Run Initialization

After the run parameters have been defined, the particle array is built as described previously. Each particle is assigned a scalar identification number and an initial velocity. The horizontal velocities vary linearly from the bottom to the top of the array, while vertical velocities are small and semi-random. The initial velocities serve the purpose of quickly breaking up the initial rectangular particle matrix into a random field, instead of wasting computer time to let the effects of the top block filter down through the array.

If the run is a restart, positions and velocities are read directly, and this step is bypassed.

### Virtual Elements and Periodic Boundaries

The next step is the creation of a set of virtual particles, one for each real moving particle, in a field adjacent to the left border of the real field. Each virtual particle is assigned an identification number the negative of that of its corresponding real particle. At each time increment each virtual particle is assigned the velocity and position of its "master." Thus the assembled real and virtual fields are as shown in Figure 3.

**Figure 3****Virtual Particles and the Virtual Field**

Interactions between negative particles are not calculated, since that would merely be repetition of what was already done in the real field.

These virtual particles don't come into play until a real particle starts to move across a boundary, as in Figure 4. Here, as soon as the center of particle (1) gets to within  $1/2$  of a diameter from the boundary, its edge is on or across the boundary line. Since now particle (-1) is now partly in the real field, it may interact with any other particle in the field, such as particle (2), as is shown. Any forces the virtual particle feels are assigned directly to its master. Thus the particle (1) in Figure 4 is in contact with both particle (2) and particle (3).



































































































































